MRC

Temperature dependence and resonance assignment of ^{13}C NMR spectra of selectively and uniformly labeled fusion peptides associated with membranes

Michele L. Bodner, Charles M. Gabrys, Paul D. Parkanzky, Jun Yang, Craig A. Duskin and David P. Weliky*

Department of Chemistry, Michigan State University, East Lansing, Michigan 48824, USA

HIV-1 and influenza viral fusion peptides are biologically relevant model fusion systems and, in this study, their membrane-associated structures were probed by solid-state NMR ^{13}C chemical shift measurements. The influenza peptide IFP-L2CF3N contained a ^{13}C carbonyl label at Leu-2 and a ^{15}N label at Phe-3 while the HIV-1 peptide HFP-UF8L9G10 was uniformly ^{13}C and ^{15}N labeled at Phe-8, Leu-9 and Gly-10. The membrane composition of the IFP-L2CF3N sample was POPC–POPG (4 : 1) and the membrane composition of the HFP-UF8L9G10 sample was a mixture of lipids and cholesterol which approximately reflects the lipid headgroup and cholesterol composition of host cells of the HIV-1 virus. In one-dimensional magic angle spinning spectra, labeled backbone ^{13}C were selectively observed using a REDOR filter of the ^{13}C–^{15}N dipolar coupling. Backbone chemical shifts were very similar at −50 and 20 °C, which suggests that low temperature does not appreciably change the peptide structure. Relative to −50 °C, the 20 °C spectra had narrower signals with lower integrated intensity, which is consistent with greater motion at the higher temperature. The Leu-2 chemical shift in the IFP-L2CF3N sample correlates with a helical structure at this residue and is consistent with detection of helical structure by other biophysical techniques. Two-dimensional ^{13}C–^{13}C correlation spectra were obtained for the HFP-UF8L9G10 sample and were used to assign the chemical shifts of all of the ^{13}C labels in the peptide. Secondary shift analysis was consistent with a β-strand structure over these three residues. The high signal-to-noise ratio of the 2D spectra suggests that membrane-associated fusion peptides with longer sequences of labeled amino acids can also be assigned with 2D and 3D methods. Copyright © 2004 John Wiley & Sons, Ltd.

KEYWORDS: NMR; ^{13}C NMR; ^{15}N NMR; HIV-1; influenza; fusion peptide; REDOR; chemical shift; assignment

INTRODUCTION

Many viruses important in disease are 'enveloped', i.e. they are enclosed by a membrane. To initiate infection of a new cell, the membranes of the virus and cell must fuse so that the viral nucleic acid can enter into the cell.[1–4] In general, there is a high activation barrier to membrane fusion and, in the absence of a catalyst, the viral–cell fusion rate is usually negligible. Fusion is also very slow between unilamellar liposomes which often serve as a model membrane system for viruses or cells. To increase the fusion rate, many enveloped viruses such as HIV-1 and influenza employ a 'fusion peptide' which represents an ~20-residue apolar domain at the N-terminus of a viral envelope fusion protein.[5,6] During fusion, this domain is

believed to interact with target cell and possibly viral membranes. Synthesized peptides with the same sequence as a fusion peptide domain will also catalyze fusion between liposomes or between red blood cells. These peptides have been the target of numerous biophysical studies and are believed to be biologically relevant model fusion systems both because of their fusogenicity and because of the good correlation between their mutagenesis–fusogenicity relationships and those of the whole viral proteins.[5] The structures of fusion peptides have been studied by solid-state NMR and other biophysical techniques and it appears that the peptides can adopt both helical and non-helical structures in membranes.[7–14] Solid-state and solution NMR methods have also been applied to study other fusion peptides which catalyze fusion between sperm and egg cells during fertilization.[15,16]

In this work, we investigated two issues related to solid-state NMR studies of membrane-associated fusion peptides. First, although physiological fusion occurs at 37 °C, many of the previous magic angle spinning (MAS) NMR measurements have been done at −50 °C because of the improved

signal-to-noise ratio at lower temperature.[13,14,17,18] In the present study, solid-state NMR spectra were obtained at both −50 and 20 °C and the spectra were compared to understand the temperature-induced changes in peptide structure and motion. Second, there has been significant recent interest in development of solid-state NMR methods to solve the structures of U-^{13}C,[15]N-labeled peptides and proteins in a manner analogous to the well-developed solution NMR techniques.[19–34] Many solid-state NMR methods are now available for sequential assignment and there is intensive effort to develop distance and torsion angle measurement techniques which are applicable to these types of samples. In the present study, we explored the feasibility of applying this type of approach to uniformly labeled fusion peptides. [13]C–[13]C 2D MAS correlation spectroscopy was applied to a membrane-associated fusion peptide which was U-^{13}C,[15]N labeled over three sequential residues. The spectra were used to determine ^{13}C chemical shifts, and the signal-to-noise ratio and resolution of the spectra were analyzed to assess the feasibility of resonance assignment and structure determination of a peptide with a much longer sequence of U-^{13}C,[15]N-labeled residues.

RESULTS

HFP-UF8L9G10 1D spectra

The HIV-1 fusion peptide HFP-UF8L9G10 (sequence AVGI-GALFLGFLGAAGSTMGARSKKK) was synthesized with the 23 N-terminal residues of the LAV$_{1a}$ strain of the HIV-1 gp41 envelope protein followed by three additional lysines for improved aqueous solubility. The HFP-UF8L9G10 peptide had U-^{13}C,[15]N labeling at Phe-8, Leu-9 and Gly-10. For the NMR sample, HFP-UF8L9G10 was associated with the 'LM3' lipid–cholesterol mixture at a peptide : lipid molar ratio of ~0.04. The LM3 mixture had the approximate lipid headgroup and cholesterol composition of host cells of the virus.[35] Figure 1 displays the Cα region of the rotational-echo double-resonance (REDOR)-filtered spectrum of the HIV-1 fusion peptide sample at (a) −50 and (b) 20 °C. Because of the 1 ms REDOR filter, the displayed spectral regions are dominated by backbone Cα signals from Phe-8, Leu-9 and Gly-10 at 53.8, 51.3 and 43.0 ppm, respectively. This assignment was made from comparison with characteristic chemical shifts and was confirmed in 2D correlation spectra (see below).[36] Corresponding peak chemical shifts agree to within 0.5 ppm at the two temperatures, indicating that the lower temperature does not induce a large peptide structural change. The carbonyl (CO) region (not displayed) was similarly invariant to temperature. The linewidths were smaller at 20 than at −50 °C. For example, for the Gly-10 peak centered at 43.0 ppm, the full width at half-maximum (FWHM) linewidth is ~2.6 ppm at −50 °C and ~1.9 ppm at 20 °C. In addition, the integrated signal-to-noise ratio per ^{13}C per transient at 20 °C is approximately one-third of its value at −50 °C. For hydrated membrane samples, it is reasonable that motion could increase significantly between −50 and 20 °C and this greater motion could explain these experimental observations. For example, increased motion could reduce inhomogeneous broadening and result in smaller linewidths.
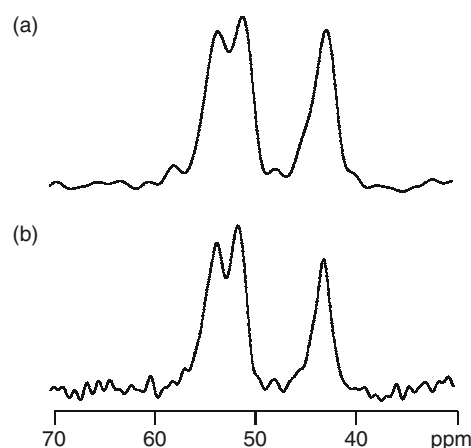

Figure 1. ^{13}C solid state NMR spectra of a sample containing HFP-UF8L9G10 peptide associated with hydrated LM3 lipid mixture at (a) −50 and (b) 20 °C. The peptide : lipid molar ratio was ~0.04, the buffer pH was 7.0 and the sample volume in the 4 mm diameter rotor was ~30 μl. The peptide had uniform ^{13}C,[15]N labeling at the Phe-8, Leu-9 and Gly-10 residues. Because of the 1 ms REDOR filter, the displayed spectral region is dominated by backbone Cα signals from Phe-8, Leu-9 and Gly-10 at 53.8, 51.3 and 43.0 ppm, respectively. For each spectrum, ^{13}C transverse magnetization was generated with [1]H–[13]C cross-polarization, the spinning speed was 8 kHz and 25 Hz Gaussian line broadening was applied. Spectrum (a) was derived from the $S_0 − S_1$ difference FID and a total of 10 496 S_0 and 10 496 S_1 transients. Spectrum (b) was similarly obtained with 82 048 S_0 and 82 048 S_1 transients. The chemical shifts are similar in spectra (a) and (b) and are consistent with non-helical structure at both −50 and 20 °C.

In addition, motion could attenuate dipolar couplings and decrease $T_{1\rho}$, which would reduce the efficiency of [1]H–[13]C cross-polarization (CP) and REDOR dephasing and result in a lower REDOR-filtered signal per ^{13}C per transient.

IFP-L2CF3N 1D spectra

The influenza fusion peptide IFP-L2CF3N (sequence GLF-GAIAGFIENGWEGMIDGGGKKKKWKWK) was synthesized with the 20 N-terminal residues of the Influenza A hemagglutinin fusion protein followed by a glycine–lysine–tryptophan sequence to improve solubility and to increase the 280 nm absorbance for analytical ultracentrifugation studies.[37] The IFP-L2CF3N peptide had a ^{13}C carbonyl label at Leu-2 and a ^{15}N label at Phe-3. For the NMR sample, IFP-L2CF3N was associated with a 1-palmitoyl-2-oleoyl-*sn*-glycero-3-phosphocholine (POPC) and 1-palmitoyl-2-oleoyl-*sn*-glycero-3-[phospho-*rac*-(1-glycerol)] (POPG) lipid mixture at a peptide : lipid molar ratio of ~0.007. This 4 : 1 POPC–POPG mixture has been used by other groups who have studied this peptide.[8,11] Figure 2 displays the carbonyl region of the REDOR-filtered spectrum of the IFP-L2CF3N sample at (a) −50 and (b) 20 °C. Because of the REDOR filter, the Leu-2 carbonyl peak dominates the spectra. The peak carbonyl shift differs by only 0.2 ppm between the two temperatures, indicating that the lower temperature does not induce a large peptide structural change. The linewidth is
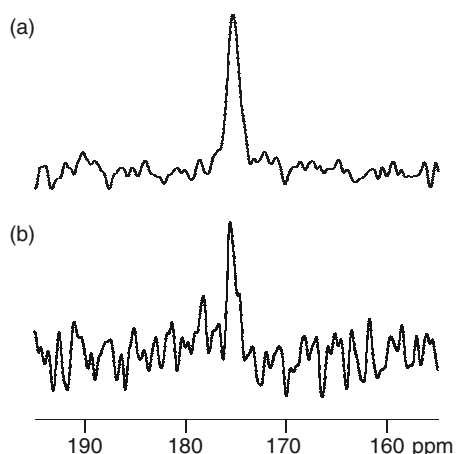
Figure 2. ^{13}C solid-state NMR spectra of a sample containing IFP-L2CF3N peptide associated with hydrated POPC/POPG (4 : 1 molar ration) lipid mixture at (a) −50 and (b) 20 °C. The peptide : lipid molar ratio was ∼0.007, the buffer pH was 5.0 and the sample volume in the 6 mm diameter rotor was ∼160 μl. The peptide had a ^{13}C carbonyl label at Leu-2 and a ^{15}N label at Phe-3. Because of the 1 ms and 4.25 ms REDOR filters in (a) and (b), respectively, only signals from the Leu-2 carbonyl are observed in the spectra. For each spectrum, the spinning speed was 8 kHz and 50 Hz Gaussian line broadening was applied. Spectrum (a) was taken with [1]H−[13]C cross-polarization and was derived from the $S_0 − S_1$ difference FID and a total of 14 796 S_0 and 14 796 S_1 transients. Spectrum (b) was taken with direct ^{13}C polarization and a total of 17 504 S_0 and 17 504 S_1 transients. In both spectra, the peak chemical shift is 175.8 ± 0.1 ppm, which is consistent with helical structure at Leu-2.

narrower at 20 than at −50 °C, and it was easier to obtain CO signals at 20 °C with direct ^{13}C polarization (DP) than with [1]H−[13]C CP. These observations are consistent with greater motion at 20 °C, and correlate with the temperature-dependent effects observed for the HFP-UF8L9G10 spectra.

In Fig. 2, the measured Leu-2 CO chemical shift of 175.8 ppm is within 0.1 ppm of the shift measured for the peptide in a frozen aqueous solution containing dodecylphosphocholine (DPC) detergent.[14] There are two lines of evidence which correlate this shift with helical structure. First, this shift is coincident with the measured 176 ppm CO shift of solid α-helical polyleucine and is very different from the 171 ppm shift of solid β-sheet polyleucine.[38,39] Second, the Leu-2 shift is within the one standard deviation (SD) range of the 176.5 ± 1.3 ppm distribution of helical Leu CO shifts in soluble proteins.[40] The Leu-2 shift fits less well with the 173.7 ± 1.5 ppm distribution for β-strand Leu CO. These distributions are derived from a chemical shift database of proteins of known structure and each distribution contains >50 shifts.

The helical solid-state Leu-2 CO shift is also consistent with solution NMR observation of helical structure near this residue for the peptide in DPC micelles and with helical structure observed for the peptide in the 4 : 1 POPC−POPG lipid mixture by electron spin resonance, infrared and circular dichroism techniques.[8,11,41,42]

In making the previously described comparison between solution and solid-state NMR chemical shifts, it was important to use the same referencing for both data sets. In the solution NMR database, shifts are referenced to ∼5 mM DSS (sodium 2,2-dimethyl-2-silapentane-5-sulfonate) at 0.0 ppm, whereas the solid state shifts are referenced to the downfield resonance of adamantane at 38.5 ppm, a secondary reference to neat tetramethylsilane (TMS) at 0.0 ppm. According to the recent measurements of Morcombe and Zilm,[43] the solution NMR reference is at −2.0 ppm relative to the solid state NMR reference. Our previously described shift comparison eliminated this referencing difference through adjustment of the solution NMR shifts.

HFP-UF8L9G10 2D spectra

Figure 3(a) displays a 2D [13]C−[13]C correlation spectrum for the HFP-UF8L9G10/LM3 sample and Fig. 3(b) displays f_2 slices from this spectrum at $f_1 = 137.6$ ppm (top) and $f_1 = 172.1$ ppm (bottom). The displayed spectra were generated from −50 °C data and the correlations were a result of magnetization exchange driven by 10 ms proton-driven spin diffusion (PDSD). A 2D correlation spectrum with similar appearance (not shown) was obtained from data for which the magnetization exchange was generated by a 4 ms radiofrequency-driven dipolar recoupling (RFDR) sequence.[44,45] Measurement of the cross-peak chemical shifts and knowledge of ^{13}C connectivities and characteristic residue-type chemical shifts made possible a full resonance assignment of all of the ^{13}C labels in the peptide. For example, the upper slice in Fig. 3(b) indicates the f_2 shifts of Phe-8 Cα, Cβ and CO by means of their correlations with the unique f_1 shift of Phe-8 aromatic C1. The full assignment is presented in Table 1. Each chemical shift entry in Table 1 is the average of between 4 and 14 f_1 and f_2 shift measurements from the PDSD and RFDR spectra. There was a typical SD of ∼0.2 ppm for the distribution of shifts used to calculate a single entry. In addition, for each nucleus, a shift (δ_{PDSD}) was calculated from only the PDSD data, a shift (δ_{RFDR}) was calculated from only the RFDR data and the shift difference Δ ($=\delta_{PDSD} − \delta_{RFDR}$) was also calculated. When all nuclei are considered, $\Delta_{average} = 0.004$ ppm and $|\Delta|_{average} = 0.2$ ppm, which indicates the absence of systematic chemical shift differences between the PDSD and RFDR data sets.

Figure 4 presents a graphical secondary shift analysis for CO, Cα and Cβ nuclei in Phe-8, Leu-9 and Gly-10, where the secondary shift is defined as the difference between

Table 1. [13]C chemical shift assignments for LM3-associated HFP-UF8L9G10[a]

	Cα	Cβ	Cγ	Cδ	Aromatic C1	Aromatic C2–6	CO
Phe-8	53.6	41.6			137.3	129.2	171.0
Leu-9	51.2	44.4	25.3	22.5			171.9
Gly-10	42.7						169.1

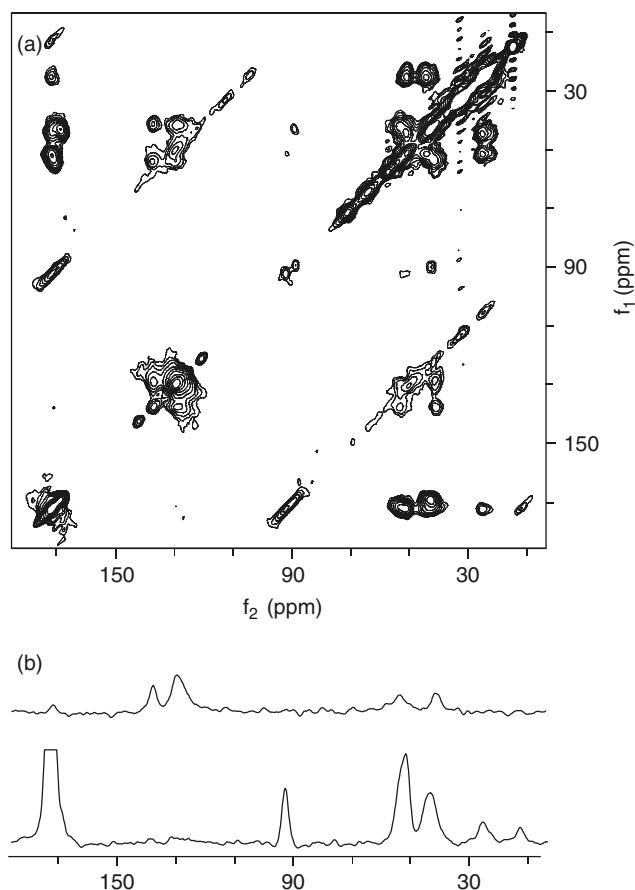[a] Chemical shifts are given in ppm and were derived from PDSD and RFDR spectra obtained at −50 °C.

Figure 3. (a) 2D ^{13}C–^{13}C contour plot spectrum of a sample containing HFP-UF8L9G10 associated with hydrated LM3 lipid mixture at $-50\,^{\circ}C$ and (b) f_2 slices from this spectrum. The peptide : lipid molar ratio was ∼0.04, the buffer pH was 7.0 and the sample volume in the 4 mm diameter rotor was ∼30 μl. The peptide had uniform ^{13}C,^{15}N labeling at the Phe-8, Leu-9 and Gly-10 residues. The 2D data were obtained with a proton-driven spin diffusion sequence and the total signal averaging time was ∼54 h. The spectrum displayed in (a) was processed with 200 Hz Gaussian line broadening in f_1 and 150 Hz line broadening in f_2. Ten contours are shown with each increasing contour representing 1.5 times greater signal intensity. In the upper slice of (b), cross peaks to the Phe-8 aromatic C1 ($f_1 = 137.6$ ppm) are displayed. From left to right, they represent magnetization in f_2 on the following Phe-8 nuclei: CO, aromatic C1 (diagonal), aromatic C2–C6, Cα and Cβ. In the lower slice of (b), cross peaks to the Leu-9 CO ($f_1 = 172.1$ ppm) are displayed. From left to right, they represent magnetization in f_2 on the following Leu-9 nuclei: CO (diagonal), CO ($m = -1$ spinning sideband), Cα, Cβ, Cγ with Cδ shoulder and CO ($m = -2$ spinning sideband).

the measured and random coil shifts. For this analysis, the literature random coil Cα and Cβ shifts[46] and CO shifts[36] were reduced by 2.1 and 2.0 ppm, respectively, which accounts for the differences between the solid-state NMR referencing to neat TMS and the solution NMR referencing to ∼5 mM 3-(trimethylsilyl)propionate (TSP) and DSS, respectively.[43,47] For the HFP-UF8L9G10 sample, the negative CO and Cα shifts and positive Cβ shifts correlate with β-strand
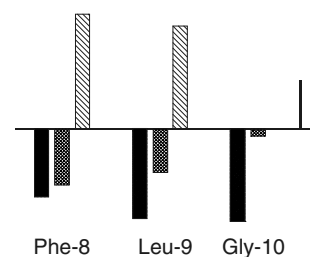

Figure 4. Secondary ^{13}C chemical shifts for Phe-8, Leu-9 and Gly-10 of HFP-UF8L9G10 associated with LM3. In each residue grouping, the secondary shifts are represented as vertical bars and are shown in left-to-right order CO, Cα, Cβ. The solid vertical line on the right is given as a scale calibration and represents a $+2$ ppm shift. For these three residues, the pattern of negative CO and Cα secondary shifts and positive Cβ shifts is diagnostic of β-strand structure.

secondary structure over these three residues.[39,40,46] Input of the chemical shifts into the TALOS secondary structure prediction program yielded Leu-9 peptide backbone (ϕ, ψ) dihedral angles of ($-130°$, $130°$).[48] These results are consistent with previous measurements of β-strand peptide backbone dihedral angles from 2D slow-spinning, rotor-synchronized MAS exchange experiments on membrane-associated HFP peptides.[13,49]

In the PDSD and RFDR spectra, (1) only intra-residue cross peaks were definitively observed and (2) relatively strong cross peaks were observed between ^{13}C separated by several bonds (e.g. Leu-9 CO/Cγ). These observations are consistent with the results of other groups using these experiments with short mixing times on U-^{13}C,^{15}N-labeled peptides and proteins.[22,26,45,50] Both PDSD and RFDR are relatively broadbanded exchange sequences mediated by ^{13}C–^{13}C dipolar coupling. For two ^{13}Cs separated by a distance r, the exchange rate will have an approximate r^{-6} dependence, and direct exchange between ^{13}Cs separated by two bonds or three bonds would occur at ∼5% or 2%, respectively, of the rate of exchange between ^{13}Cs separated by one bond. Hence it is more likely that a two- or three-bond cross peak is due to multiple steps of exchange between directly bonded ^{13}Cs rather than a single-step exchange process. With the assumption that there is a single rate constant for directly bonded ^{13}C exchange, at short times the ratio of intensities of the two-bond/one-bond cross peaks will be about the same as the ratio of three-bond/two-bond cross peaks and the ratio of four-bond/three-bond cross peaks. This model is qualitatively supported by the relative intensities of the cross peaks in the slices in Fig. 3(b). For example, in the lower slice, the relative intensities of the Leu-9 CO/Cα, CO/Cβ, CO/Cγ and CO/Cδ cross peaks are ∼10:6:2:1 and all of the $(n+1)$-bond/n-bond cross-peak intensity ratios are within a range of 0.3–0.6. Inter-residue cross peaks are likely not observed in these short mixing time spectra because the ^{15}N interrupts the direct ^{13}C bond network. Inter-residue cross peaks are apparent in a 2D PDSD spectrum with a longer 100 ms mixing time (data not shown), in accord with the experience of other investigators.[50]

DISCUSSION

Temperature dependence of the spectra

Viral–target cell membrane fusion occurs at 37 °C, but for membrane-associated HFP and IFP samples, the signal-to-noise ratio per peptide ^{13}C per transient is about three times higher at −50 than at 20 °C (cf Figs 1 and 2). It is therefore advantageous to obtain ^{13}C NMR spectra of these samples at −50 °C. It is also important to demonstrate the biological relevance of the cold samples and to therefore investigate whether cooling changes the peptide structure. For both the HFP and IFP samples, the chemical shifts are similar at 20 and −50 °C, which suggests that cooling does not change the average peptide structure. The temperature dependences of intensities and linewidths suggest that motion at 20 °C is attenuated at −50 °C, which is a physically reasonable result for hydrated membrane samples.

In the future, it will be interesting to measure peptide chemical shifts at 37 °C, the physiological fusion temperature, and to compare them with the shifts at −50 and 20 °C. It is also useful to consider lipid properties at −50, 20 and 37 °C. Because of the presence of 33 mol% cholesterol in LM3, the lipids in the HFP/LM3 sample are probably in a fluid lamellar phase at 20 and 37 °C and in a lamellar glass at −50 °C.[17,51] The liquid crystalline to gel phase transitions of both POPC (PC) and POPG (PG) occur at ∼0 °C, so for the IFP/PC/PG sample, the lipids are probably in the liquid crystalline phase at 20 and 37 °C and in the gel phase at −50 °C.[52] We note that although the lipid phases probably will not change between 20 and 37 °C, there will probably be greater lipid and peptide motion with this increase in temperature.

Fusion peptide structural plasticity

Interestingly, the chemical shift data obtained in this and previous solid-state NMR studies suggest that LM3-associated HFP is predominantly non-helical, whereas PC/PG-associated IFP is predominantly helical in its N-terminal region.[13,14] This difference in structure exists at both 20 and −50 °C, which implies that cooling the sample does not cause conversion of helical to non-helical structure or vice versa. The solid-state NMR results on IFP are consistent with helical structure observed for the peptide in DPC detergent by solution NMR and with helical structure observed for the peptide in PC/PG by electron spin resonance, infrared and circular dichroism techniques.[8,11,37,41,42]

There are several possible explanations for the observed structural difference between the HFP and IFP samples. First, the samples have different peptide : lipid molar ratios, 0.04 and 0.007, respectively. However, this difference in ratios is probably not the most important reason for the structural difference, as previous measurements of the Phe-8 CO chemical shift in LM3-associated HFP samples have demonstrated shift and presumably structural invariance over the molar ratio range 0.005 ≤ peptide : lipid ≤ 0.05.[13] A second possibility is that the structural difference is due to differences between the HFP and IFP amino acid sequences. If this were the case, then LM3-associated IFP should be helical and PC/PG-associated HFP should be non-helical. However, preliminary chemical shift measurements on these types of samples do not support this hypothesis and suggest that the main structural determinant for either peptide is the lipid and cholesterol composition of the membrane. For example, studies by our group suggest that IFP adopts a mixture of helical and non-helical structure when associated with membranes composed of PC, PG and cholesterol.[14] This observation of peptide plasticity has also been made by other investigators using techniques other than solid-state NMR.[5,10,53−55] With application of functional fusion assays to peptides interacting with different membrane compositions, it may be possible to elucidate the relative fusogenicities of the helical and non-helical structures. Preliminary data from our group suggest that fusion may be induced by either structure.

Prospects for assignment and structure determination of U-^{13}C,^{15}N-labeled fusion peptides

There has been significant recent interest in the development of solid-state NMR methods for assignment and structure determination of U-^{13}C,^{15}N-labeled peptides and proteins. There has been great progress in assignment methods and the structure determination methods are an area of active research. This paper describes a pilot study of the application of these methods to membrane-associated fusion peptides. We are encouraged by our results, in particular the high signal-to-noise of the 9.4 T 2D spectrum of a sample containing only ∼0.3 μmol of peptide. It is reasonable to expect that 2D ^{15}N–^{13}C correlation experiments will also work on these systems and, with a somewhat longer signal averaging time, 3D ^{15}N–^{13}C–^{13}C correlation experiments are also viable. These experiments will probably be useful for sequential assignment through application of selective ^{15}N–^{13}Cα or ^{15}N–^{13}CO transfers.[56−58] Because of the 2−3 ppm ^{13}C linewidths and the presence of six glycines and five alanines in the HFP sequence, 3D methods may be required to do a unique assignment for the fully labeled peptide. For the next step of the experimental work, we have synthesized a fusion peptide which is U-^{13}C,^{15}N-labeled over 12 sequential residues and have begun the assignment experiments. As with any U-^{13}C,^{15}N-labeled system, it is expected that doing experiments at higher field will improve both the signal-to-noise ratio and the resolution of the spectra because of larger population differences and attenuation of ^{13}C–^{13}C J-couplings, respectively.[59]

EXPERIMENTAL

Materials

Rink amide resin was purchased from Advanced Chemtech (Louisville, KY, USA) and 9-fluorenylmethoxycarbonyl (FMOC)-amino acids from Peptides International (Louisville, KY, USA). Isotopically labeled amino acids were purchased from either Cambridge (Andover, MA, USA) or Icon (Summit, NJ, USA) and were FMOC-protected using literature procedures. 1-Palmitoyl-2-oleoyl-*sn*-glycero-3-phosphocholine (POPC), 1-palmitoyl-2-oleoyl-*sn*-glycero-3-phosphoethanolamine (POPE), 1-palmitoyl-2-oleoyl-*sn*-glycero-3-(phospho-L-serine) (POPS), phosphatidylinositol (PI), sphingomyelin and 1-palmitoyl-2-oleoyl-*sn*-glycero-3-[phospho-*rac*-(1-glycerol)] (POPG) were purchased from

Avanti Polar Lipids (Alabaster, AL, USA). The Micro BCA protein assay was obtained from Pierce (Rockford, IL, USA). *N*-2-Hydroxyethylpiperazine-*N'*-2-ethanesulfonic acid (HEPES) and Triton X-100 were obtained from Sigma. All other reagents were of analytical grade.

Peptides

HFP-UF8L9G10 fusion peptide (sequence AVGIGALFLGFL-GAAGSTMGARSKKK) was synthesized with the 23 N-terminal residues of the LAV$_{1a}$ strain of the HIV-1 gp41 envelope protein followed by three additional lysines for improved solubility. IFP-L2CF3N fusion peptide (sequence GLFGAIAGFIENGWEGMIDGGGKKKKWKWK) was synthesized with the 20 N-terminal residues of the Influenza A hemagglutinin fusion protein followed by a glycine–lysine–tryptophan sequence to improve solubility and to increase the 280 nm absorbance for analytical ultra-centrifugation studies.[37] Both peptides were synthesized as their C-terminal amides using a Model 431A peptide synthesizer (ABI, Foster City, CA, USA) equipped for FMOC chemistry. HFP-UF8L9G10 had uniform ^{13}C,^{15}N labeling at the Phe-8, Leu-9 and Gly-10 residues and IFP-L2CF3N was ^{13}C carbonyl labeled at Leu-2 and amide ^{15}N labeled at Phe-3.

HFP-UF8L9G10 peptide concentrations in aqueous solution were quantitated using the BCA assay and IFP-L2CF3N peptide concentrations were quantitated by measuring the absorbance at 280 nm. The assays were calibrated with quantitative amino acid analysis. For IFP-L2CF3N, this calibration yielded an extinction coefficient of ~20 000 l mol^{-1} cm^{-1}.

Solid-state NMR sample preparation

Membrane-associated peptide samples were prepared as described previously.[13,14] Two different membrane compositions were used: (1) 'LM3' which had POPC, POPE, POPS, sphingomyelin, PI and cholesterol in a 10 : 5 : 2 : 2 : 1 : 10 molar ratio and (2) 'PC/PG' which had POPC and POPG in a 4 : 1 molar ratio. PC/PG has been used by other investigators while the LM3 composition reflects the approximate lipid headgroup and cholesterol content of membranes of host cells of the HIV virus.[8,11,35] The HFP and IFP samples were prepared in 5 mM HEPES buffer (pH 7.0) and 10 mM acetate buffer (pH 5.0), respectively, which reflect the approximate fusion pHs for the HIV-1 and influenza viruses. In the sample preparation protocol, an ~30 ml peptide solution was prepared which contained ~1.6 µmol of peptide for the HFP sample and ~0.4 µmol of peptide for the IFP sample. Analytical ultracentrifugation data were consistent with predominantly monomeric peptide in these solutions (J. Yang, P. D. Parkanzky, M. Prorok, F. J. Castellino, M. Lemmon and D. P. Weliky, unpublished work). An ~5 ml volume of solution was then prepared which contained extruded ~150 nm diameter unilamellar vesicles (LUVs). For the HFP sample, the LUV solution contained ~40 µmol of total lipid and ~20 µmol of cholesterol, and for the IFP sample, the LUV solution contained ~50 µmol of total lipid. The peptide and LUV solutions were mixed and kept at room temperature overnight. The mixed solution was then ultracentrifuged at 100 000 − 130 000*g* for 4–5 h to pellet the LUVs and associated bound peptide. Nearly all peptide binds to LUVs under

these conditions, and unbound peptide does not pellet. A portion of the peptide–LUV pellet formed after ultracentrifugation was transferred by spatula to a MAS NMR rotor. The total pellet volume was ~200 µl.

The rotor was sealed with a vespel end-cap which had been pre-cooled in liquid nitrogen prior to insertion into the rotor. At liquid nitrogen temperature, the cap fitted snugly in the rotor. When the cap warmed, it formed a very tight seal with the rotor, which minimized dehydration of the sample.

NMR spectroscopy

In peptide–membrane samples containing specifically ^{13}C-labeled peptide, the direct-polarized (DP) or ^{1}H–^{13}C cross-polarized (CP) ^{13}C NMR spectra typically have very large lipid, cholesterol and peptide natural abundance signals. In this study, two approaches were taken to filter out the natural abundance signals. For 1D spectra, a rotational-echo double-resonance (REDOR) NMR filtering sequence was applied and the resulting spectra were dominated by labeled backbone ^{13}C with directly bonded ^{15}N.[14,60] For the IFP-L2CF3N sample a clean spectrum of the Leu-2 carbonyl (CO) was observed and for the HFP-UF8L9G10 sample a clean spectrum was observed of the Phe-8, Leu-9 and Gly-10 Cα and the Phe-8 and Leu-9 CO carbons. In the second filtering approach, 2D ^{13}C–^{13}C correlation spectra were obtained on the HFP-UF8L9G10 sample and off-diagonal cross peaks were only detected between labeled ^{13}Cs.

The NMR spectra were taken on 9.4 T spectrometers (Infinity Plus, Varian, Palo Alto, CA, USA) using triple resonance MAS probes equipped for either 4 mm diameter rotors (HFP-UF8L9G10 sample) or 6 mm diameter rotors (IFP-L2CF3N sample). The temperature was monitored by a thermocouple located about 1 in from the rotor and in the flow of the cooling nitrogen gas. The actual temperature of the sample is probably higher than the measured temperature because of frictional heating from sample spinning and from heating due to the radiofrequency (r.f.) fields. In the NMR probe circuit, the r.f. fields are highly attenuated at the ends of the coil and it was observed experimentally that nearly all of the NMR signal comes from the central two-thirds of the sample volume specified by the manufacturer. Hence, in the 6 mm rotor, longer spacers were used to restrict samples to this central two-thirds volume (~160 µl). For the 4 mm rotor, the total possible rotor sample volume was ~70 µl. The rotor was opened at the end of the MAS experiments and it was estimated that the actual volume of sample was ~30 µl.

The detection channel was tuned to ^{13}C at 100.2 or 100.8 MHz, the decoupling channel was tuned to ^{1}H at 398.6 or 400.8 MHz and the third channel for REDOR-filtered 1D spectra was tuned to ^{15}N at 40.4 or 40.6 MHz. ^{13}C chemical shift referencing was done using the methylene resonance of solid adamantane at 38.5 ppm.[43] The ^{15}N transmitter was set to ~115 ppm using solid (^{15}NH$_4$)$_2$SO$_4$ as a chemical shift reference at 20 ppm. The ^{13}C π pulse r.f. field, ^{1}H π/2 pulse field, ^{1}H and ^{13}C CP fields and ^{15}N π pulse field were set using model compounds. For the HFP-UF8L9G10 sample the model compound was leucine containing 5% U-^{13}C,^{15}N-labeled molecules diluted in natural abundance material

and for the IFP-L2CF3N sample the model compound was a lyophilized 25-residue peptide with a directly bonded ^{13}C carbonyl/^{15}N amide pair. The MAS frequency was 8000 ± 2 Hz.

REDOR-filtered 1D experiments

For the 1D experiments, generation of ^{13}C transverse magnetization was followed by a REDOR dephasing period and then direct ^{13}C detection. For the HFP-UF8L9G10 sample, the ^{13}C transmitter was set to 155 ppm at $-50\,^{\circ}$C and to 100 ppm at $20\,^{\circ}$C. ^{13}C transverse magnetization was generated using ^{1}H–^{13}C CP with a 53–57 kHz ^{13}C ramp and 1.8 ms contact time at $-50\,^{\circ}$C and 3 ms contact time at $20\,^{\circ}$C. The dephasing period was set to eight rotor periods (1 ms) and contained a single 55 kHz ^{13}C refocusing π pulse at the center of this period. For the S_1 acquisition, 45 kHz ^{15}N π pulses were applied at the middle and end of every rotor cycle during the dephasing period except for the fourth and eighth cycles. The S_0 acquisition did not contain these ^{15}N π pulses. In the dephasing period, pulse timing was not actively synchronized to the rotor position. Two-pulse phase modulation (TPPM) ^{1}H decoupling at 100 kHz was applied during both dephasing and detection with 5.4 µs pulse length and 90° and 105° phases.[61] To obtain optimal compensation of B_0, B_1 and MAS frequency drifts, S_0 and S_1 free induction decays (FIDs) were acquired alternately. The recycle delay was 2 s at $-50\,^{\circ}$C and 1.3 s at $20\,^{\circ}$C.

A Z-filter sequence was used to set the ^{13}C π pulse length and contained the following sequential elements: ^{1}H–^{13}C CP; ^{13}C $\pi/2$; 10 ms; ^{13}C π; detection. ^{1}H decoupling was applied during pulses and detection. The ^{15}N π pulse length was set by minimization of S_1 signals for the model compound and the TPPM pulse length was set by maximization of the S_0 signal for the model compound.

For each S_1 transient, XY-8 phase cycling was applied to the ^{15}N π pulses.[62,63] Individual S_0 or S_1 transients were coadded with the following phase cycling scheme: ^{1}H $\pi/2$, $x, -x, x, -x$; ^{13}C CP and ^{13}C $\pi, -y, -y, x, x$; receiver, $x, -x, y, -y$. After completion of data acquisition, the sum of S_1 FIDs was subtracted from the sum of S_0 FIDs. Spectral processing was done on the difference FID with a DC offset correction, 25 Hz Gaussian line broadening, Fourier transformation and baseline correction.

The set-up, spectrometer parameters and processing parameters were similar for the IFP-L2CF3N sample at $-50\,^{\circ}$C with the following adjustments: 153 ppm ^{13}C transmitter; 38–62 kHz ^{13}C CP ramp over a 1.4 ms contact time; 50 kHz ^{13}C and ^{15}N π pulse r.f. fields, 75 kHz ^{1}H decoupling field; 7.4 µs ^{1}H TPPM pulse length; 2 s recycle delay; 50 Hz line broadening. For the IFP-L2CF3N sample at $20\,^{\circ}$C, initial attempts to obtain a REDOR difference signal were unsuccessful, so we used a different REDOR pulse program which employed direct ^{13}C polarization (DP) rather than ^{1}H–^{13}C CP. In addition, the REDOR dephasing period was set to 34 rotor periods (4.25 ms) and contained a ^{15}N π pulse in the middle of every rotor cycle and a ^{13}C π pulse at the end of each rotor cycle except for the last cycle.[64] Relative to the 1 ms dephasing period of the $-50\,^{\circ}$C experiment, a longer dephasing period was used at $20\,^{\circ}$C to reflect the possibility

that there is some motional averaging of the ^{13}C–^{15}N dipolar coupling. The alternating ^{15}N/^{13}C π pulse rather than the single ^{13}C π pulse version of REDOR was chosen because for longer dephasing times, the former version gives more overall signal than the latter version[65] (J. Yang and D. P. Weliky, unpublished work). This result may be due to better refocusing of chemical shifts over two rotor cycles relative to many rotor cycles. Relative to $-50\,^{\circ}$C, other changed spectrometer parameters in the $20\,^{\circ}$C IFP-L2CF3N experiment were the 155 ppm ^{13}C transmitter, 40 kHz ^{15}N π pulse r.f. field, 65 kHz ^{1}H decoupling field and 5 s recycle delay. Individual S_0 or S_1 transients were co-added with the following phase cycling scheme: ^{13}C $\pi/2$, $x, y, -x, -y$; ^{13}C π, $y, -x, -y, x$; receiver, $x, y, -x, -y$, where ^{13}C π refers to the last ^{13}C π pulse during the dephasing period. For each S_1 transient, the ^{15}N π pulses followed an XY-8 phase cycle, and for each S_0 and S_1 transient, the first 32 ^{13}C π pulses followed an XY-8 phase cycle.

2D experiments

The 2D ^{13}C–^{13}C correlation spectra were obtained on the HFP-UF8L9G10 sample at $-50\,^{\circ}$C with the probe configured for double resonance ^{13}C/^{1}H operation. The ^{13}C sensitivity in double resonance mode was $\sim$1.5 times greater than the sensitivity in triple resonance mode. For one data set, correlations were generated by the proton-driven spin diffusion (PDSD) pulse sequence $CP - t_1 - \pi/2 - \tau - \pi/2 - t_2$, where t_1 was the evolution period, the first $\pi/2$ pulse rotated ^{13}C transverse magnetization to the longitudinal axis, τ was a 10 ms spin diffusion period during which ^{13}C longitudinal magnetization was transferred between ^{13}C nuclei connected by a network of direct ^{13}C–^{13}C bonds, the second $\pi/2$ pulse rotated ^{13}C longitudinal magnetization to the transverse plane and t_2 was the detection period. Continuous-wave (CW) ^{1}H decoupling at 100 kHz was applied during the pulse, t_1 and t_2 periods, but not during τ. In a second data set, longitudinal transfer of ^{13}C magnetization during τ was achieved with use of the r.f.-driven dipolar recoupling (RFDR) method.[44,45] In this approach, a ^{13}C π pulse was applied at the end of rotor cycles 1, 3, 5, . . ., 31 during τ. CW ^{1}H decoupling at 100 kHz was also applied during τ. The τ period contained a total of 32 rotor cycles. The following parameters were common to the PDSD and RFDR data sets: 8 kHz MAS frequency; 44–64 kHz ramp on the ^{13}C CP r.f. field; 2 ms CP contact time; 50 kHz ^{13}C $\pi/2$ pulse r.f. field; 25 µs t_1 dwell time; 20 µs t_2 dwell time; and 1 s recycle delay. Hypercomplex data were obtained by acquiring two individual FIDs for each t_1 point with either a ^{13}C $(\pi/2)_x$ or $(\pi/2)_y$ pulse at the end of the t_1 evolution period. For the first of these t_1 FIDs, individual transients were coadded with the following phase cycling scheme: first ^{13}C $\pi/2$ pulse, $x, -x, x, -x, x, -x, x, -x$; second ^{13}C $\pi/2$ pulse, $x, x, y, y, -x, -x, -y, -y$; receiver, $y, -y, -x, x, -y, y, x, -x$. For the other t_1 FID, the first ^{13}C $\pi/2$ pulse followed $y, -y, y, -y, y, -y, y, -y$ cycling. The PDSD data were acquired in $\sim$54 h with 120 t_1 points, 512 t_2 points and 768 transients per FID, and the RFDR data were acquired in $\sim$60 h with 200 t_1 points, 1024 t_2 points and 512 transients per FID. Both data sets were processed according to the

method of States using nmrPipe software.[66,67] Processing included zero-filling, Gaussian line broadening and baseline correction. After double Fourier transformation, the PDSD spectrum was composed of 1024 $(f_1) \times 2048(f_2)$ data points with 39 Hz (f_1) and 24 Hz (f_2) digital resolution.

Acknowledgments

REFERENCES

1. Blumenthal R, Dimitrov DS. In *Membrane Fusion*; Hoffman JF, Jamieson JC (eds). Oxford University Press: New York, 1997; 563–603.
2. Dimitrov DS. *Cell* 2000; **101**: 697.
3. Epand RM. *Biosci. Rep.* 2000; **20**: 435.
4. Blumenthal R, Clague MJ, Durell SR, Epand RM. *Chem. Rev.* 2003; **103**: 53.
5. Durell SR, Martin I, Ruysschaert JM, Shai Y, Blumenthal R. *Mol. Membr. Biol.* 1997; **14**: 97.
6. Eckert DM, Kim PS. *Annu. Rev. Biochem.* 2001; **70**: 777.
7. Nieva JL, Nir S, Muga A, Goni FM, Wilschut J. *Biochemistry* 1994; **33**: 3201.
8. Macosko JC, Kim CH, Shin YK. *J. Mol. Biol.* 1997; **267**: 1139.
9. Curtain C, Separovic F, Nielsen K, Craik D, Zhong Y, Kirkpatrick A. *Eur. Biophys. J.* 1999; **28**: 427.
10. Han X, Tamm LK. *J. Mol. Biol.* 2000; **304**: 953.
11. Han X, Bushweller JH, Cafiso DS, Tamm LK. *Nat. Struct. Biol.* 2001; **8**: 715.
12. Epand RM, Epand RF, Martin I, Ruysschaert JM. *Biochemistry* 2001; **40**: 8800.
13. Yang J, Gabrys CM, Weliky DP. *Biochemistry* 2001; **40**: 8126.
14. Yang J, Parkanzky PD, Bodner ML, Duskin CG, Weliky DP. *J. Magn. Reson.* 2002; **159**: 101.
15. Glaser RW, Grune M, Wandelt C, Ulrich AS. *Biochemistry* 1999; **38**: 2560.
16. Ulrich AS, Afonin SE, Glaser RW, Duerr U, Salgado J, Grage SL, Berditchevskaia M, Wadhwani P. *Biophys. J.* 2002; **82**: 2502.
17. Yang J, Parkanzky PD, Khunte BA, Canlas CG, Yang R, Gabrys CM, Weliky DP. *J. Mol. Graph. Model.* 2001; **19**: 129.
18. Yang R, Yang J, Weliky DP. *Biochemistry* 2003; **42**: 3527.
19. Marassi FM, Ramamoorthy A, Opella SJ. *Proc. Natl. Acad. Sci. USA* 1997; **94**: 8551.
20. Straus SK, Bremi T, Ernst RR. *J. Biomol. NMR* 1998; **12**: 39.
21. Hong M, Jakes K. *J. Biomol. NMR* 1999; **14**: 71.
22. McDermott A, Polenova T, Bockmann A, Zilm KW, Paulsen EK, Martin RW, Montelione GT. *J. Biomol. NMR* 2000; **16**: 209.
23. Marassi FM, Opella SJ. *J. Magn. Reson.* 2000; **144**: 150.
24. Wang J, Denny J, Tian C, Kim S, Mo Y, Kovacs F, Song Z, Nishimura K, Gan Z, Fu R, Quine JR, Cross TA. *J. Magn. Reson.* 2000; **144**: 162.
25. Detken A, Hardy EH, Ernst M, Kainosho M, Kawakami T, Aimoto S, Meier BH. *J. Biomol. NMR* 2001; **20**: 203.
26. Pauli J, Baldus M, van Rossum B, de Groot H, Oschkinat H. *ChemBioChem* 2001; **2**: 272.
27. Egorova-Zachernyuk TA, Hollander J, Fraser N, Gast P, Hoff AJ, Cogdell R, de Groot HJM, Baldus M. *J. Biomol. NMR* 2001; **19**: 243.
28. Denny JK, Wang JF, Cross TA, Quine JR. *J. Magn. Reson.* 2001; **152**: 217.
29. Mesleh MF, Veglia G, DeSilva TM, Marassi FM, Opella SJ. *J. Am. Chem. Soc.* 2002; **124**: 4206.
30. Rienstra CM, Tucker-Kellogg L, Jaroniec CP, Hohwy M, Reif B, McMahon MT, Tidor B, Lozano-Perez T, Griffin RG. *Proc. Natl. Acad. Sci. USA* 2002; **99**: 10 260.
31. Castellani F, van Rossum B, Diehl A, Schubert M, Rehbein K, Oschkinat H. *Nature (London)* 2002; **420**: 98.
32. Lange A, Luca S, Baldus M. *J. Am. Chem. Soc.* 2002; **124**: 9704.
33. Petkova AT, Baldus M, Belenky M, Hong M, Griffin RG, Herzfeld J. *J. Magn. Reson.* 2003; **160**: 1.
34. Marassi FM, Opella SJ. *Protein Sci.* 2003; **12**: 403.
35. Aloia RC, Tian H, Jensen FC. *Proc. Natl. Acad. Sci. USA* 1993; **90**: 5181.
36. Wishart DS, Bigam CG, Holm A, Hodges RS, Sykes BD. *J. Biomol. NMR* 1995; **5**: 67.
37. Han X, Tamm LK. *Proc. Natl. Acad. Sci. USA* 2000; **97**: 13 097.
38. Kricheldorf HR, Muller D. *Macromolecules* 1983; **16**: 615.
39. Saito H. *Magn. Reson. Chem.* 1986; **24**: 835.
40. Zhang HY, Neal S, Wishart DS. *J. Biomol. NMR* 2003; **25**: 173.
41. Dubovskii PV, Li H, Takahashi S, Arseniev AS, Akasaka K. *Protein Sci.* 2000; **9**: 786.
42. Hsu CH, Wu SH, Chang DK, Chen CP. *J. Biol. Chem.* 2002; **277**: 22 725.
43. Morcombe CR, Zilm KW. *J. Magn. Reson.* 2003; **162**: 479.
44. Bennett AE, Ok JH, Griffin RG, Vega S. *J. Chem. Phys.* 1992; **96**: 8624.
45. Bennett AE, Rienstra CM, Griffiths JM, Zhen WG, Lansbury PT, Griffin RG. *J. Chem. Phys.* 1998; **108**: 9463.
46. Spera S, Bax A. *J. Am. Chem. Soc.* 1991; **113**: 5490.
47. Wishart DS, Bigam CG, Yao J, Abildgaard F, Dyson HJ, Oldfield E, Markley JL, Sykes BD. *J. Biomol. NMR* 1995; **6**: 135.
48. Cornilescu G, Delaglio F, Bax A. *J. Biomol. NMR* 1999; **13**: 289.
49. Gabrys CM, Yang J, Weliky DP. *J. Biomol. NMR* 2003; **26**: 49.
50. Straus SK, Bremi T, Ernst RR. *J. Biomol. NMR* 1997; **10**: 119.
51. Bloom M, Evans E, Mouritsen OG. *Q. Rev. Biophys.* 1991; **24**: 293.
52. Caffrey M. *LIPIDAT: a Database of Thermodynamic Data and Associated Information on Lipid Mesomorphic and Polymorphic Transitions*, CRC Press: Boca Raton, FL, 1993.
53. Martin I, Schaal H, Scheid A, Ruysschaert JM. *J. Virol.* 1996; **70**: 298.
54. Davies SMA, Kelly SM, Price NC, Bradshaw JP. *FEBS Lett.* 1998; **425**: 415.
55. Saez-Cirion A, Nieva JL. *Biochim. Biophys. Acta Biomembr.* 2002; **1564**: 57.
56. Baldus M, Geurts DG, Hediger S, Meier BH. *J. Magn. Reson. A* 1996; **118**: 140.
57. Baldus M, Petkova AT, Herzfeld J, Griffin RG. *Mol. Phys.* 1998; **95**: 1197.
58. Rienstra CM, Hohwy M, Hong M, Griffin RG. *J. Am. Chem. Soc.* 2000; **122**: 10 979.
59. Straus SK, Bremi T, Ernst RR. *Chem. Phys. Lett.* 1996; **262**: 709.
60. Gullion T, Schaefer J. *J. Magn. Reson.* 1989; **81**: 196.
61. Bennett AE, Rienstra CM, Auger M, Lakshmi KV, Griffin RG. *J. Chem. Phys.* 1995; **103**: 6951.
62. Gullion T, Baker DB, Conradi MS. *J. Magn. Reson.* 1990; **89**: 479.
63. Gullion T, Schaefer J. *J. Magn. Reson.* 1991; **92**: 439.
64. McDowell LM, Holl SM, Qian SJ, Li E, Schaefer J. *Biochemistry* 1993; **32**: 4560.
65. Anderson RC, Gullion T, Joers JM, Shapiro M, Villhauer EB, Weber HP. *J. Am. Chem. Soc.* 1995; **117**: 10 546.
66. States DJ, Haberkorn RA, Ruben DJ. *J. Magn. Reson.* 1982; **48**: 286.
67. Delaglio F, Grzesiek S, Vuister GW, Zhu G, Pfeifer J, Bax A. *J. Biomol. NMR* 1995; **6**: 277.